

DTIC FILE COPY

4

AD-A199 131

AFGL-TR-88-0094

INFLUENCE OF SCATTERING ON SEISMIC WAVES:
VELOCITY AND ATTENUATION STRUCTURE OF THE UPPER CRUST IN SOUTHEAST
MAINE

Edmund Reiter
M. Nafi Toksöz
Anton M. Dainty

Earth Resources Laboratory
Department of Earth, Atmospheric, and
Planetary Sciences
Massachusetts Institute of Technology
Cambridge, Massachusetts 02139

21 March 1988

Scientific Report No. 3

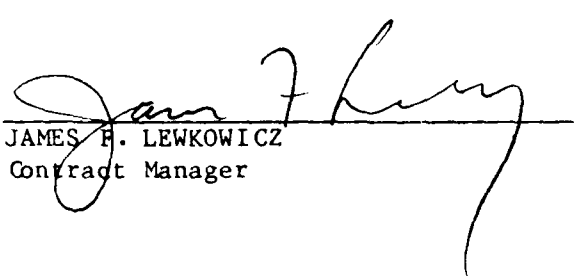
APPROVED FOR PUBLIC RELEASE; DISTRIBUTION UNLIMITED

Air Force Geophysics Laboratory
Air Force Systems Command
United States Air Force
Hanscom Air Force Base, Massachusetts 01731

DTIC
ELECTE
SEP 07 1988
E

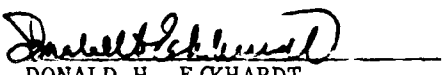
88 9 8 15 1

"This technical report has been reviewed and is approved for publication."


JAMES F. LEWKOWICZ
Contract Manager


HENRY A. OSSING
Chief, Solid Earth Geophysics Branch

FOR THE COMMANDER


DONALD H. ECKHARDT
Director
Earth Sciences Division

This report has been reviewed by the ESD Public Affairs Office (PA) and is releasable to the National Technical Information Service (NTIS).

Qualified requestors may obtain additional copies from the Defense Technical Information Center. All others should apply to the National Technical Information Service.

If your address has changed, or if you wish to be removed from the mailing list, or if the addressee is no longer employed by your organization, please notify AFGL/DAA, Hanscom AFB, MA 01731. This will assist us in maintaining a current mailing list.

Do not return copies of this report unless contractual obligations or notices on a specific document requires that it be returned.

ADA199131

REPORT DOCUMENTATION PAGE

1a REPORT SECURITY CLASSIFICATION Unclassified			1b RESTRICTIVE MARKINGS	
2a SECURITY CLASSIFICATION AUTHORITY			3 DISTRIBUTION/AVAILABILITY OF REPORT Approved for public release; distribution unlimited	
2b DECLASSIFICATION/DOWNGRADING SCHEDULE				
4 PERFORMING ORGANIZATION REPORT NUMBER(S)			5 MONITORING ORGANIZATION REPORT NUMBER(S) AFGL-TR-88-0094	
6a NAME OF PERFORMING ORGANIZATION Earth Resources Laboratory Dept. of Earth, Atmospheric, and Planetary Sciences	6b OFFICE SYMBOL (if applicable)	7a NAME OF MONITORING ORGANIZATION Air Force Geophysics Laboratory		
6c ADDRESS (City, State, and ZIP Code) Massachusetts Institute of Technology Cambridge, MA 02139		7b ADDRESS (City, State, and ZIP Code) Hanscom AFB, MA 01731		
8a NAME OF FUNDING/SPONSORING ORGANIZATION	8b OFFICE SYMBOL (if applicable)	9 PROCUREMENT INSTRUMENT IDENTIFICATION NUMBER F19628-86-K-0004		
8c ADDRESS (City, State, and ZIP Code)		10 SOURCE OF FUNDING NUMBERS		
		PROGRAM ELEMENT NO 61101E	PROJECT NO 6A10	TASK NO DA
		WORK UNIT ACCESSION NO BF		
11 TITLE (Include Security Classification) Influence of Scattering on Seismic Waves: Velocity and Attenuation Structure of the Upper Crust in Southeast Maine (unclassified)				
12 PERSONAL AUTHOR(S) M. Nafi Toksöz, Edmund Reiter, Anton M. Dainty				
13a TYPE OF REPORT Scientific Report No. 3	13b TIME COVERED FROM 2/1/87 TO 7/31/87	14 DATE OF REPORT (Year, Month, Day) 1988 March 21	15 PAGE COUNT 60	
16 SUPPLEMENTARY NOTATION				
17 COSATI CODES			18 SUBJECT TERMS (Continue on reverse if necessary and identify by block number)	
FIELD	GROUP	SUB-GROUP		
			Rg, anisotropy, crustal structure, attenuation, New England, refraction profile.	
19 ABSTRACT (Continue on reverse if necessary and identify by block number) Rg and Pg velocities and Rg attenuation have been examined for the Central Merrimack Synclinorium and nearby regions in southeastern Maine using digital records from a seismic refraction experiment. Determination of Rg group velocities and Pg travel times indicates that both lateral variations and azimuthal anisotropy are present in the study area. The axes of the azimuthal velocity anisotropy appear to lie along and perpendicular to the Appalachian structural strike in the region, with Pg group velocities along strike up to 20% faster than cross strike velocities. Measurement of Rg attenuation gives Q values of 1.4-1.7, varying with frequency. Inversion of the Rg group velocity for velocity structure shows that both the compressional and shear velocities increase rapidly with depth in the upper 1 km in the region.				
20 DISTRIBUTION/AVAILABILITY OF ABSTRACT <input checked="" type="checkbox"/> UNCLASSIFIED/UNLIMITED <input type="checkbox"/> SAME AS RPT <input type="checkbox"/> DTIC USERS			21 ABSTRACT SECURITY CLASSIFICATION unclassified	
22a NAME OF RESPONSIBLE INDIVIDUAL James P. Leskovicz			22b TELEPHONE (Include Area Code) 617/477-3028	22c OFFICE SYMBOL LWH

TABLE OF CONTENTS

INTRODUCTION	1
DATA	3
ANALYSIS	6
GROUP VELOCITY OBSERVATIONS	9
Lateral Variation in Velocity Structure	10
Azimuthal Dependence of Group Velocity	12
ATTENUATION OBSERVATIONS	19
INVERSION	27
CONCLUSIONS	35
REFERENCES	36

Accession For	
NTIS GRA&I	<input checked="" type="checkbox"/>
DTIC TAB	<input type="checkbox"/>
Unannounced	<input type="checkbox"/>
Justification	
By _____	
Distribution/	
Availability Codes	
Avail and/or	
Dist	Special
A-1	



INTRODUCTION

Short period Rayleigh waves (Rg) provide a convenient tool for studying the elastic properties of the upper crust. Group and phase velocities of Rg waves are particularly sensitive to variations in upper crustal shear wave velocity structure, and two station surface wave attenuation methods may be used to study the anelastic properties of the upper few kilometers of the crust. Despite many crustal geophysical studies, the shear wave velocity structure of the upper few kilometers of the crust remains relatively poorly constrained. Refraction experiments are generally concerned with deeper structure while reflection work usually involves only compressional velocities. Laboratory shear velocities using ultrasonic techniques have been measured for many of the rocks commonly found in the upper crust but may fail to adequately reproduce *in situ* conditions such as partial closure of cracks and incomplete saturation.

Near surface seismic sources such as quarry and refraction blasts are efficient generators of Rg waves. In New England, local networks archive hundreds of digital seismograms from quarry blasts every year. Typically the Rg phase is the largest amplitude arrival on the seismogram and is observable to approximately 100 km, depending on the size of the blast and the nature of the travel path. Recent crustal refraction surveys represent another sizeable source of digitally recorded short period Rayleigh waves. The density of receivers in a typical crustal refraction survey (one station per 1-2 km) provides an excellent geometry for correlating Rg velocities, and therefore shear velocity structure, with surficial sedimentary deposits and mapped bedrock units.

A number of investigators have used Rg dispersion to study upper crustal velocity structure. Kafka and Dollin (1985) used the dispersion of 0.5-2 Hz Rg waves to map lateral variations in

velocity structure in Connecticut. Båth (1975) observed normally dispersed Rg in the 0.5–2 Hz frequency range and concluded there was a general increase in velocity with depth in the upper 1–3 km of the crust. Anderson and Dorman (1973) studied the effects of surficial sedimentary deposits on 0.6–5 Hz Rayleigh waves in the New York City area. With the exception of Al-Husseini *et al.* (1981), previous studies involve sparse data sets with quarry blasts or small shallow earthquakes as sources and sparse local networks as receivers. Al-Husseini *et al.* (1981) calculated phase velocities of 10–30 Hz fundamental mode Rayleigh waves from f-k transforms of seismic reflection spreads in northern Saudi Arabia. The large volume of data allowed the mapping of 150,000 km² and correlation of phase velocity with various surficial sedimentary units.

This study focuses on determining the velocity and attenuation structure of the upper crust from Rg arrivals recorded in the 5–30 km distance range. Velocity profiles are obtained by an iterative, least squares, maximum likelihood inversion of group velocity observations; additional constraints on velocity structure include observation of Pg velocities. The density and geometry of group velocity observations in this study allow an in depth study of the behavior of velocity structure as a function of distance. Attenuation measurements using the two station method show relatively little scatter compared with other upper crustal attenuation studies (Pulli, 1983). Some problems with this method of determining attenuation with Rg waves are identified.

DATA

The data for this study are from a refraction survey conducted in Maine by the United States Geological Survey (Murphy and Luetgert, 1986,1987). The survey, conducted in the fall of 1984, was part of a broad-based geophysical investigation of the northern Appalachian Mountains that included seismic reflection, gravity and magnetic studies. Principal goals of these studies include an accurate mapping of Moho depth, identification of major intercrustal discontinuities and investigation of the complex region of a major plate collision that portions of Maine are commonly thought to represent.

The refraction survey consisted of 8 separate lines of 120 instruments, each approximately 90 km long and laid out as shown in Figure 1. Data from deployments 3, 4, 5 and 6 were obtained from the USGS and deployments 5 and 6 were selected for processing and study primarily on the basis of the authors' interests. The major structural feature of the study area is the Central Merrimack Synclinorium. Instrument and shot locations and elevations were determined using USGS 1:24,000 and 1:62,500 topographic maps and are assumed accurate to within 20 m. Shots consisted of 2000 lb of ammonium nitrate explosive located in a 20cm by 40m drill hole; shot times are assumed accurate to within ± 2 msec. Figure 2 shows three seismograms representative of the data used in this study.

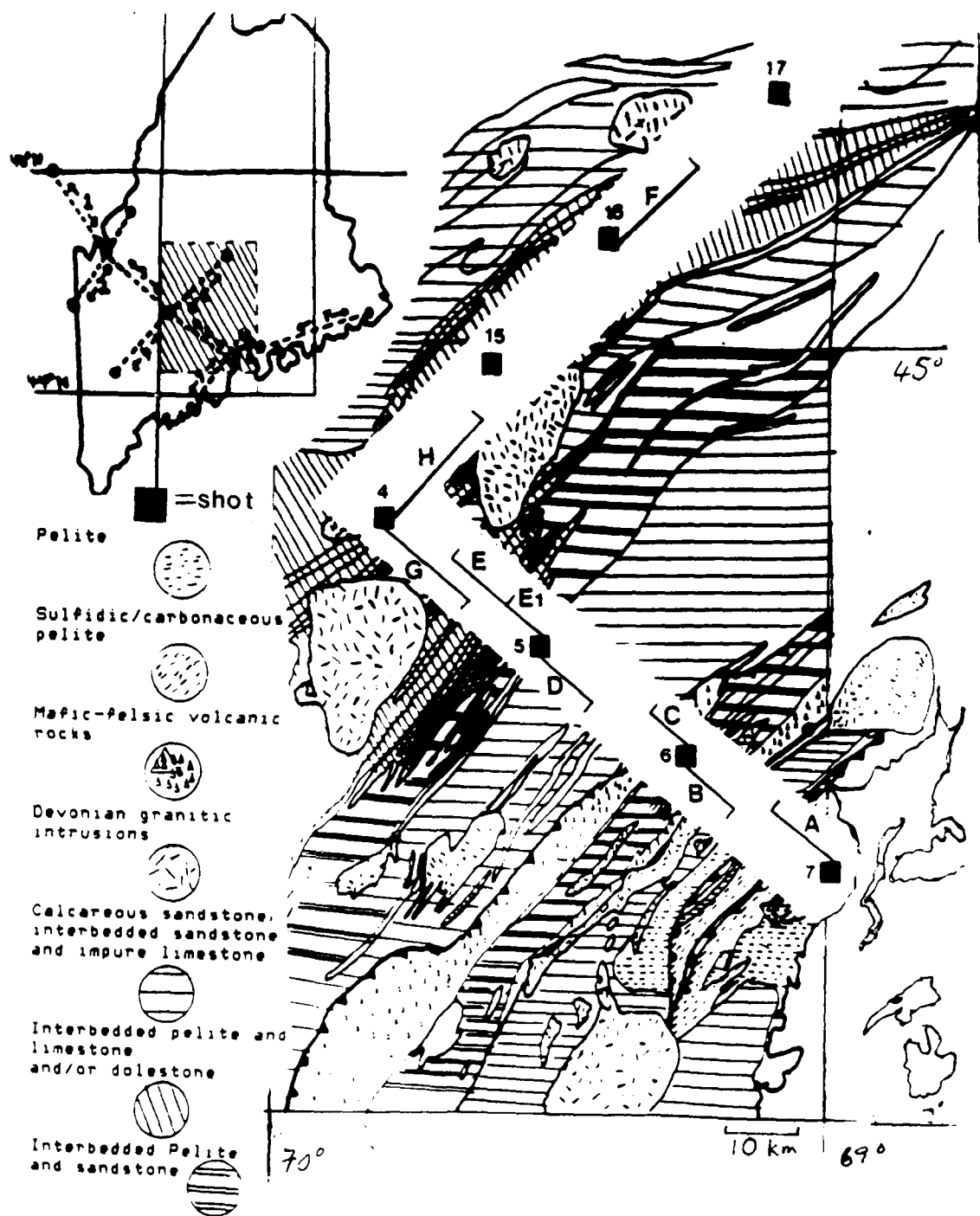


Figure 1. Map of general area and regions of study.

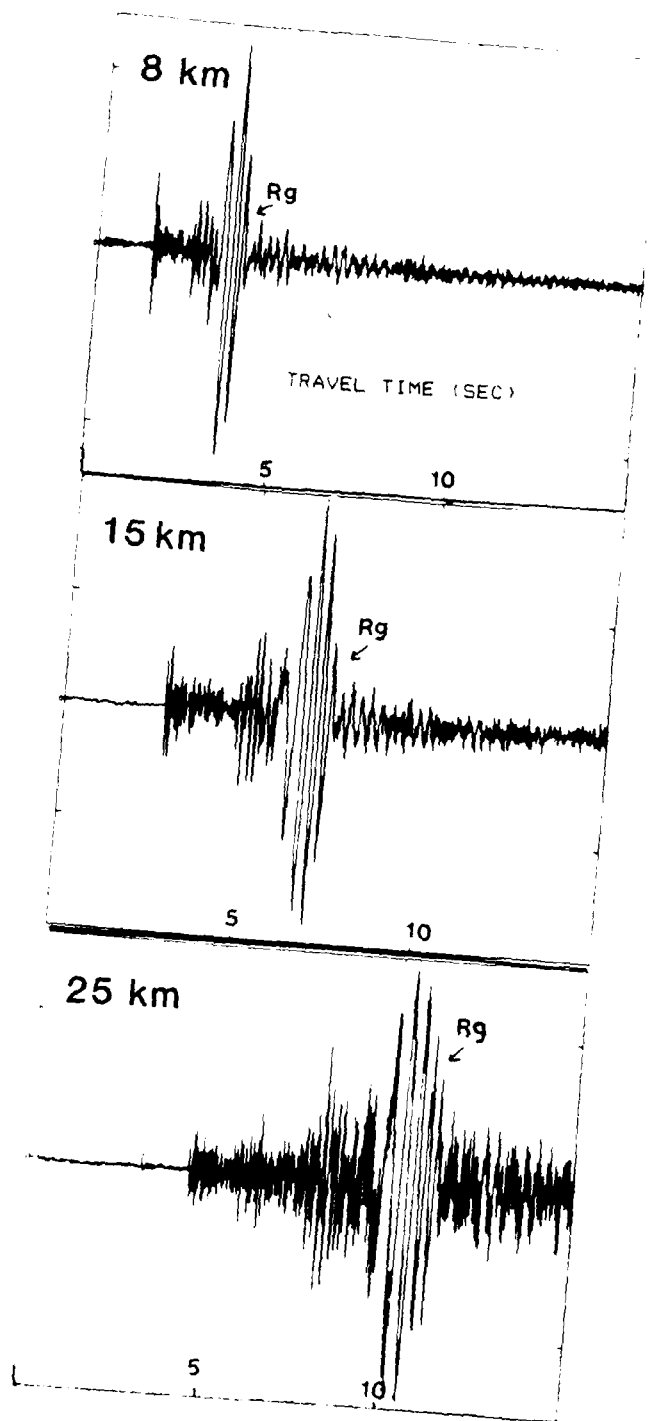


Figure 2. Typical seismograms recorded at 8, 15 and 25 km offsets. Amplitudes adjusted for display purposes.

ANALYSIS

Group velocities were determined using the multiple narrow bandpass filter technique described by Dziewonski and Hales (1972). Originally designed primarily for analysis of 20–200 second period Rayleigh waves, this technique worked well for the range of periods in this study. A brief description of the more important aspects of this technique is given below.

A Gaussian function

$$H(\omega) = e^{-\alpha(\frac{\omega - \omega_c}{\omega_c})^2} \quad (1)$$

is chosen to represent the filter transfer function. This filter is chosen because of the mutual properties of its time and frequency durations. If we express the RMS time and frequency durations of a general signal as

$$(\mathcal{D}_t)^2 = \int_{-\infty}^{\infty} t^2 |f(t)|^2 dt \quad (2)$$

and

$$(\mathcal{D}_\omega)^2 = \int_{-\infty}^{\infty} \omega^2 |F(\omega)|^2 d\omega \quad (3)$$

it can be shown that the value of the product of the RMS durations for the Gaussian function, $(\mathcal{D}_t \cdot \mathcal{D}_\omega)$, is the least of all the possible non-band limited functions, being equal to the constant $\sqrt{\pi/2}$ (Papoulis, 1962). This means that the frequency-time resolution, commonly measured as $1/(\mathcal{D}_t \cdot \mathcal{D}_\omega)$, is greater for a Gaussian filter than for any other non-band limited filter.

Representing the seismogram as

$$F(\omega) = A(\omega) \cdot e^{i(k(\omega)r - \omega t)} \quad (4)$$

and using first order Taylor expansions for $A(\omega)$ and $k(\omega)$ it can be shown that the maximum

amplitude of the filtered signal, given a filter of the form described above, corresponds to the group travel time of the energy associated with the frequency ω_c (Dziewonski *et al.*, 1969). The seismogram is repeatedly filtered with appropriate values of ω_c and α and a group velocity dispersion curve derived from the peak amplitudes of the filtered envelopes.

Attenuation as a function of frequency was measured from the decay of Rg spectra recorded at distances between 10 and 30 km. The Rg arrival was windowed in the time domain and an amplitude spectrum calculated from the window. If $A(\omega, r_1)$ and $A(\omega, r_2)$ represent the amplitude spectra of two receivers at r_1 and r_2 , and $U(\omega)$ the interstation group velocity of the Rg wave, $Q(\omega)$ may be calculated as (Ben-Menahem and Singh, 1981)

$$Q(\omega) = \omega / (2 \cdot \gamma(\omega) \cdot U(\omega)) \quad (5)$$

with

$$\gamma(\omega) = \frac{\ln[A(\omega, r_1)/A(\omega, r_2)]}{(r_1 - r_2)} \quad (6)$$

Pg velocities were calculated by picking the arrival time of the phase, subtracting the known origin time to find the travel time and dividing the source-receiver distance by the travel time. Pg arrival times are accurate since at distances relevant to this study, 5–30 km, Pg is the first arrival and has an impulsive onset.

An iterative least squares maximum likelihood inverse routine was used to invert the group velocity observations for crustal velocity structure (Menke, 1984). A formulation by Rodi *et al.* (1975) was used to calculate partial derivatives of group velocity from partial derivatives of phase velocity. This formulation requires the calculation of a double set of roots and phase-velocity partials to obtain the group-velocity partials for all model parameters at a given frequency. It is

ultimately based on the derivative relationship between group and phase velocity. The necessary phase velocity, group velocity and phase velocity partial derivative calculations were carried out using techniques described in Takeuchi and Saito (1972). In this procedure variational principles are used to formulate expressions for group velocity and phase velocity partial derivatives which involve energy integrals and not numerical differentiation. This results in a more accurate determination of group velocity and a much quicker method of obtaining the phase velocity partial derivatives.

GROUP VELOCITY OBSERVATIONS

Approximately 400 seismograms were analyzed for Rg group velocity dispersion using the multiple filter technique discussed previously. As shown in Figure 1, source-receiver distances ranged from 5-30 km, and station spacing averaged one station per 800 m. We have chosen to focus on two features of the dispersion data. First, lateral variations in group velocity with group velocity differences of 0.25-0.35 km/sec are found and appear to correlate in some cases with mapped bedrock units and possibly tectonic features. Second, a dependence of group velocity on azimuth is observed. Pg velocities are consistent with both of the above observations. Before discussing these observations we will briefly examine some limitations and problems involved in the interpretation of Rg and Pg velocities.

Fundamental resolution problems involving primarily wavelength and receiver density limit the use of Rg waves in delineating regions of similar dispersive properties. Examples presented here involve regions of roughly 10 km in length; assuming wavelengths ranging from 0.5-3 km, and receiver spacing of one recorder per 800 m, the wavelengths and receiver density are of proper size to adequately sample these areas. When interpreting Pg velocities for crustal velocity structure it is important to consider the difficulty in constraining the ray path of this phase. Pg ray paths in this distance range are very sensitive to the compressional velocity gradient in the upper 2 km of the crust, and given the lack of distinct refractor legs on the travel time curves calculation of absolute crustal velocities from these arrivals is difficult. However, by comparing Pg velocities calculated at similar offsets in different regions the differences in ray paths is hopefully minimized, thus providing a reasonable quantity with which to compare velocity structures. In any event, if

the Pg velocities measured as described above are different at the same offset for two regions, we may certainly say that the structure is different.

Lateral Variation in Velocity Structure

Lateral variation in velocity structure was studied using group velocities measured for paths cutting the structural trend at approximately 90°. Group velocities for the six regions marked A, B, C, D, E and G were measured by calculating group velocities for three receivers located at the end of each boundary marked on Figure 1. Receiver spacing averaged about one receiver per 800 meters so the three group velocity measurements shown for each region are all located within a kilometer of the end of the marked boundaries.

Variations in Rg group velocity of 0.25–0.35 km/sec were observed between the fastest and slowest paths in this area (Figure 3). The fastest velocities were observed for region G which consists of about half calcareous sandstone and impure limestone, and half interbedded pelite and limestone. The slowest velocities were recorded about 50 km away in region B. This region is composed primarily of interbedded pelite and sandstone with minor amounts of mafic-felsic volcanics and calcareous sandstone. In regions G and B group velocities appear to be associated with lithology but this is usually not the case. Regions A, D and E have nearly identical group velocities (Figure 3) yet have travel paths composed of distinctly different lithologies. Region A consists almost entirely of sulfidic/carbonaceous pelite while region D consists of calcareous sandstone and impure limestone. Region E is composed of about half interbedded pelite and sandstone and half interbedded pelite and dolomite. These three regions (A, D and E) all have group velocities ranging from around 2.55 km/sec at 1 Hz to 2.35 km/sec at 5 Hz yet include almost every lithology found

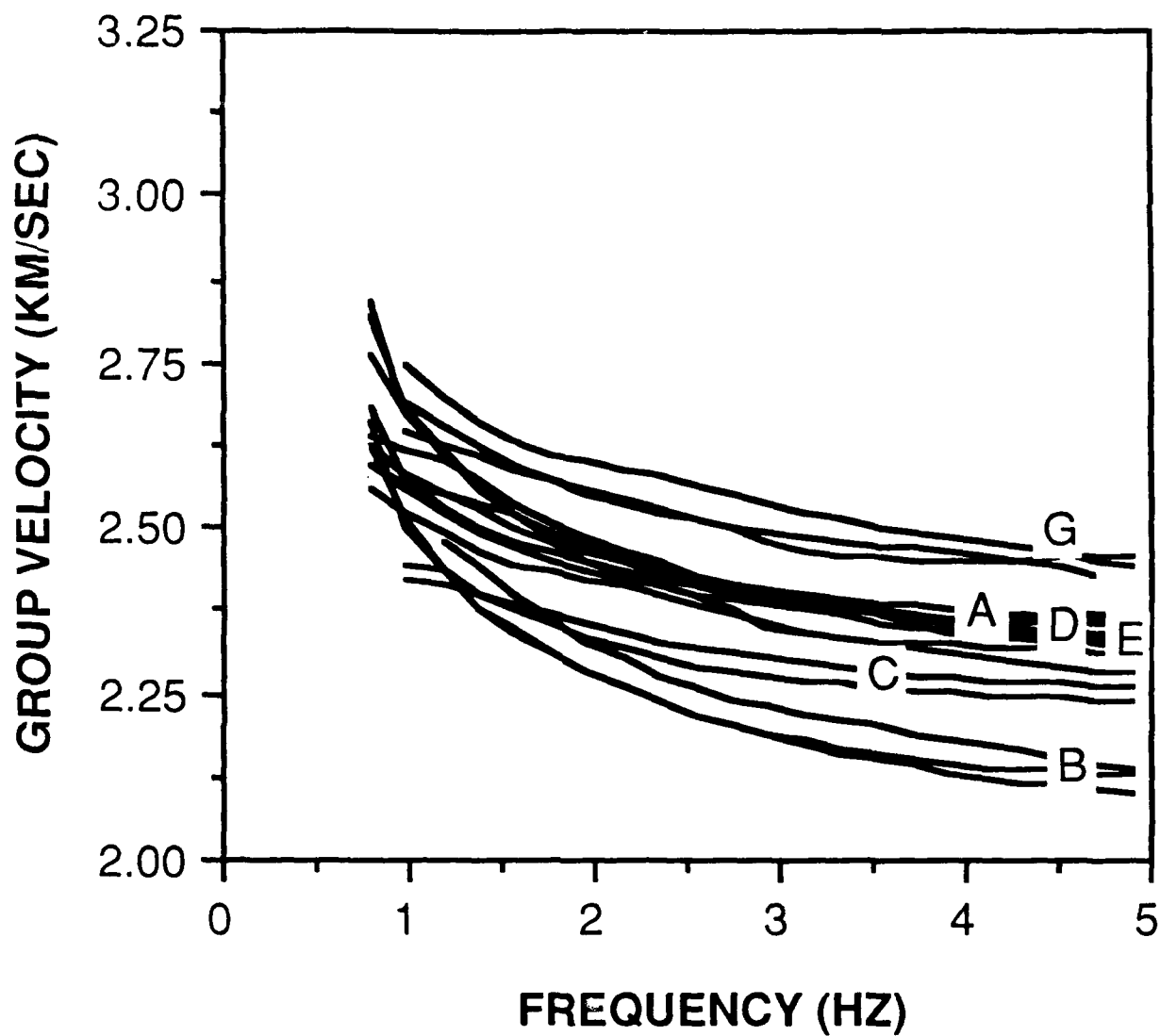


Figure 3. Group velocities for regions A, B, C, D, E and G. Note evidence for lateral variation in velocity structure.

in the region. Regions A and B are composed of different units and also are separated by a thrust fault. As is illustrated in Figure 3 these regions differ in group velocity by around 0.2 km/sec. This suggests that Rg group velocities might be helpful in delineating this tectonic boundary. In general, group velocities for cross strike paths vary from 2.4–2.6 km/sec at 1 Hz to 2.1–2.45 km/sec at 5 Hz. In some cases different lithologies are observed to display different Rg dispersive characteristics while in others the opposite is true.

Pg velocities were calculated for each of the regions discussed above. At the offsets relevant to these regions, 5–20km, Pg ray paths bottom at a maximum depth of around 2 km and especially at offsets near 20 km may be sampling slightly deeper velocity structure than the Rg waves. An average Pg velocity for a given region was determined by averaging Pg velocities determined at each of the three stations used in the previously discussed group velocity analysis. Table 1 lists these velocities and the offsets at which they were calculated. In general the Pg velocities show a similar lateral variation in velocity structure but require further analysis such as ray tracing and travel time curve modeling in order to fully utilize this information. Such analysis is beyond the scope of this study and Pg velocities are presented only to provide a qualitative means of velocity structure comparison.

Azimuthal Dependence of Group Velocity

A dependence of Rg group velocity on azimuth was observed for all paths within the Central Merrimack Synclinorium. Faster velocities were observed for paths nearly parallel to the structural trend of the region and slower velocities for paths perpendicular to this direction. To illustrate this azimuthal dependence of group velocity, we will first examine four specific regions and then all

Table 1: Pg velocities showing differences between regions

Region	Offset (km)	Velocity (km/sec)
A	8	5.70
A	17	5.75
B	8	5.40
B	17	5.65
C	6	5.40
C	10	5.45
D	6	5.45
D	10	5.50
E	15	5.38
G	15	5.60

relevant data as a function of azimuth. Pg velocities will also be compared and used to substantiate the group velocity observations.

Figure 4 compares the group velocities for regions E and F. Both regions consist primarily of interbedded pelite, limestone and sandstone and have little (less than 150 m per 5 km) topographic variation. Thus, although over 90 km apart, regions E and F are of similar composition and topography, and can be expected to exhibit similar dispersion characteristics. Figure 4, however, shows a 15% difference in group velocities for the two regions. The group velocities measured for region E were calculated with an interstation method in order to more accurately measure the velocity of the pelite-limestone-sandstone unit by eliminating the effects of the portion of the path labeled E1. Pg velocities measured at a 15 km offset differed by 0.7 km/sec or 12%. However, the effect of E1 is present in the 15 km offset Pg velocity calculation. The group velocity of E1 is found to be slightly less than that of E, and thus is expected to bias the Pg velocity calculated in E downward, in effect increasing the difference between regions F and E. This effect is sufficiently

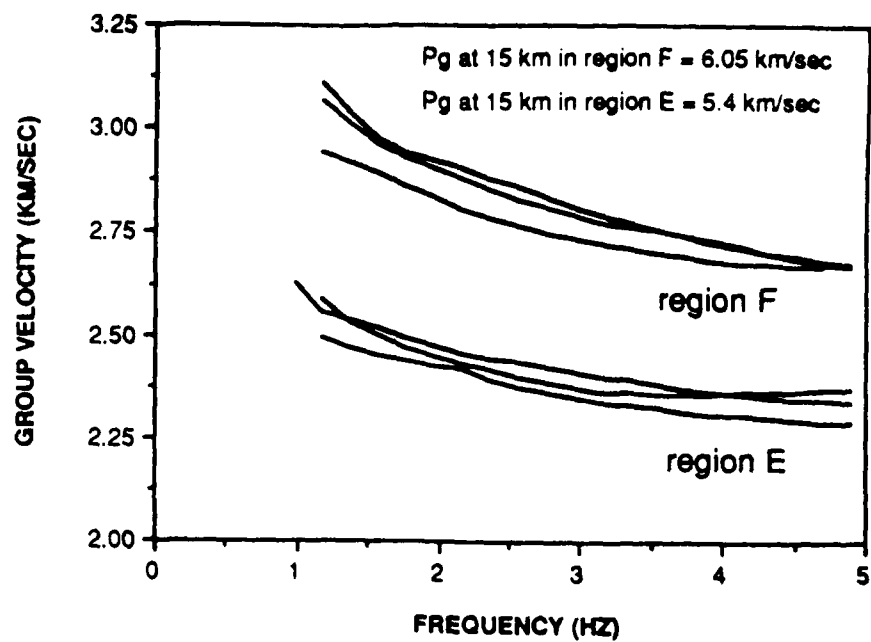


Figure 4. Group velocities for regions E and F.

small and well known to allow a valid comparison of Pg velocities between regions E and F and indicates that a difference of 10% is probably more representative of the actual *in situ* Pg velocities for these path geometries.

Group velocities for regions G and H are shown in Figure 5. As in all previous examples Pg velocities show the same trend as the Rg velocities; an Rg group velocity difference of 18% and a Pg velocity difference of 7% is observed for these two regions. These velocity differences between regions G and H provide some of the strongest evidence of an azimuthal dependence of velocity. As in the comparison of regions E and F, the mapped bedrock units in each region are quite similar. However unlike regions E and F which are approximately 90 km apart, G and H are adjacent to one another. The proximity of G and H combined with the compositional and topographic similarities suggest strongly that lateral variation in velocity structure is not the principal cause of the observed velocity differences.

Figure 6 is a plot of group velocity from several azimuths for paths entirely within the Central Merrimack Synclinorium. Although azimuthal coverage is sparse, group velocities measured from shot #16 in region F which cuts the structural grain at approximately 20° lie between the minimum (cross strike) and maximum (along strike) observations. Previous geophysical studies such as gravity surveys, seismic reflection and structural interpretations have failed to produce any evidence of the elongate, high velocity structure needed to explain the observed velocities with a laterally varying model. The apparent dependence of velocity on azimuth coupled with the lack of evidence for a laterally varying structure lead us to suggest a model requiring an anisotropic crust in at least the upper 2 km and probably significantly deeper. Symmetry axes of the anisotropy appear to

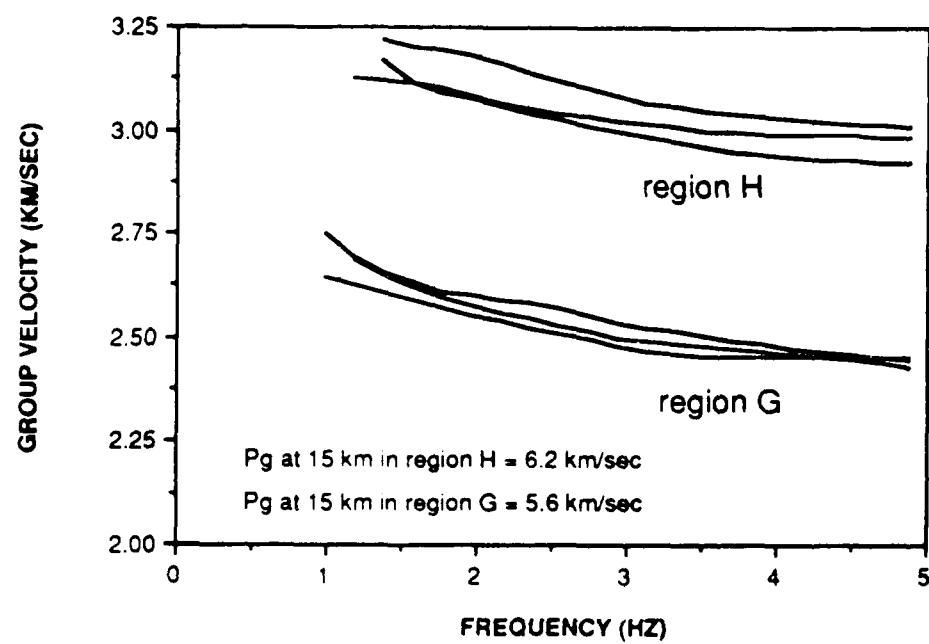


Figure 5. Group velocities for regions G and H.

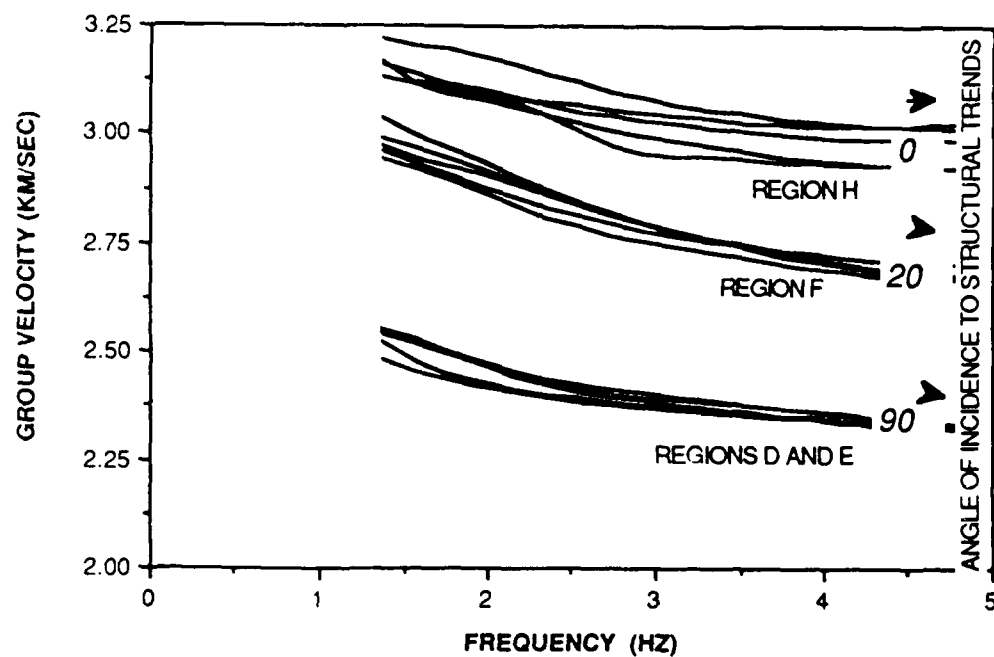


Figure 6: Group velocities from Central Merrimack Synclinorium with angle of incidence with respect to gross structural trends

be determined by the orientation of the structural trend of the region which is approximately N30°E. Further analysis of the orientation of the symmetry axes involved is not possible with the azimuthally limited velocity observations of this study.

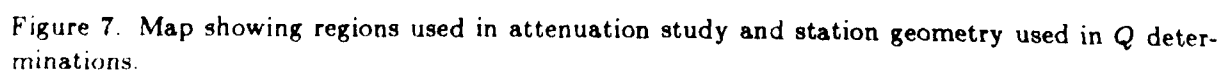
ATTENUATION OBSERVATIONS

The attenuation structure of the upper crust was studied using the surface wave $Q(\omega)$ analysis method discussed earlier. Difficulties with this method, arising primarily from suspected lateral variations/anisotropy in velocity structure, are identified and an average $Q(\omega)$ is determined from selected portions of the data set. $Q(\omega)$ calculated in this manner is found to be too unstable a quantity for use in delineating the individual attenuation properties of specific bedrock units, but provides a reasonable measure of the gross attenuation structure of the upper crust.

In the previously discussed formulation (5) and (6) for $Q(\omega)$ the implicit assumption is made that the difference between the two spectra $A(\omega, r_1)$ and $A(\omega, r_2)$, after correction for geometrical spreading, is due solely to the effect of dissipation of seismic energy. In a laterally homogeneous, isotropic, medium this is indeed the case and provided the exponential decay law is valid relations (5) and (6) provide a simple method for measuring $Q(\omega)$ from surface wave spectra. If, however, the structure has significant lateral velocity variation or anisotropy, the spectral difference observed between r_1 and r_2 is due not only to the effect of attenuation but also to the lateral change/anisotropy in velocity structure. Scattering from a sharp vertical velocity boundary (Chen and Alsop, 1979), fundamental to higher mode conversion (Kennett, 1984), multipathing (Yomogida 1985), and a different surface wave spectral response to the new medium must all be considered in the presence of lateral velocity variation and anisotropy. By averaging $Q(\omega)$ observations from many different regions we try to minimize the problem of lateral heterogeneity and feel reasonably confident that the $Q(\omega)$ values presented are representative of the gross attenuation properties of the upper crust, although the effect of anisotropy remains to be quantified.

An average $Q(\omega)$ was determined for regions J, K and L in Figure 7. Receiver separation averaged approximately 10 km with 9 station pairs used in the determination of an average Q for each region. The parts of the profiles labeled "1" in Figure 7 are the locations of the near receivers (r_2); the far receivers are located in the other part of the profiles. This source-receiver geometry has the effect of minimizing structural effects unique to an individual receiver while providing the redundancy necessary in attenuation studies. The spectra used for region J are shown in Figure 8. The investigation in this region suggests that lateral heterogeneities are a substantial problem when determining $Q(\omega)$ with the two station surface wave method. Group velocity curves for J and J1 are shown in Figure 8 and show a significant lateral variation in velocity structure. The dashed curve in Figure 8 is the group velocity curve used in the Q determination. It was determined by measuring the interstation group velocity between the three stations at approximately 15 km range and the three stations at approximately 25 km range. Also, there are large and very rapid variations of Q as a function of frequency for frequencies greater than 3.5 Hz. Such variations cannot be explained by a change of the average Q with depth because the Q at two nearly identical frequencies would be nearly the same, i.e., there is a limit to the rapidity of Q variations with frequency due to such a structure. For this reason we suspect that lateral heterogeneity is playing a role.

Regions K and K1 (Figures 7, 9) represent another area in which lateral changes in velocity structure are suspected of causing substantial contamination of $Q(\omega)$ calculations. Group velocities measured for K and K1 again show a lateral variation in velocity structure. Also, spectra from the 14-16 km range (K1) lack the well developed "notch" near 2.5 Hz seen in spectra from the 24-26 km range. The large peak in Q at 2.5 Hz is caused by this difference, and for the same reasons as



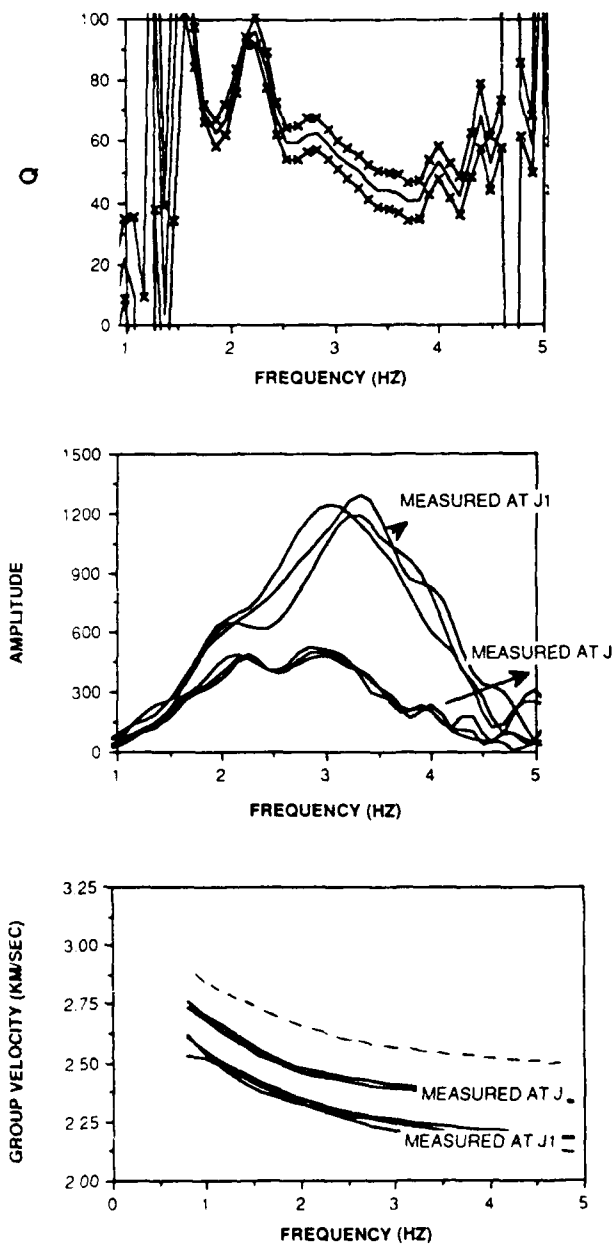


Figure 8. $Q(\omega)$, spectra and group velocities for regions J and J1. Dashed curve is the interstation group velocity used for Q determination.

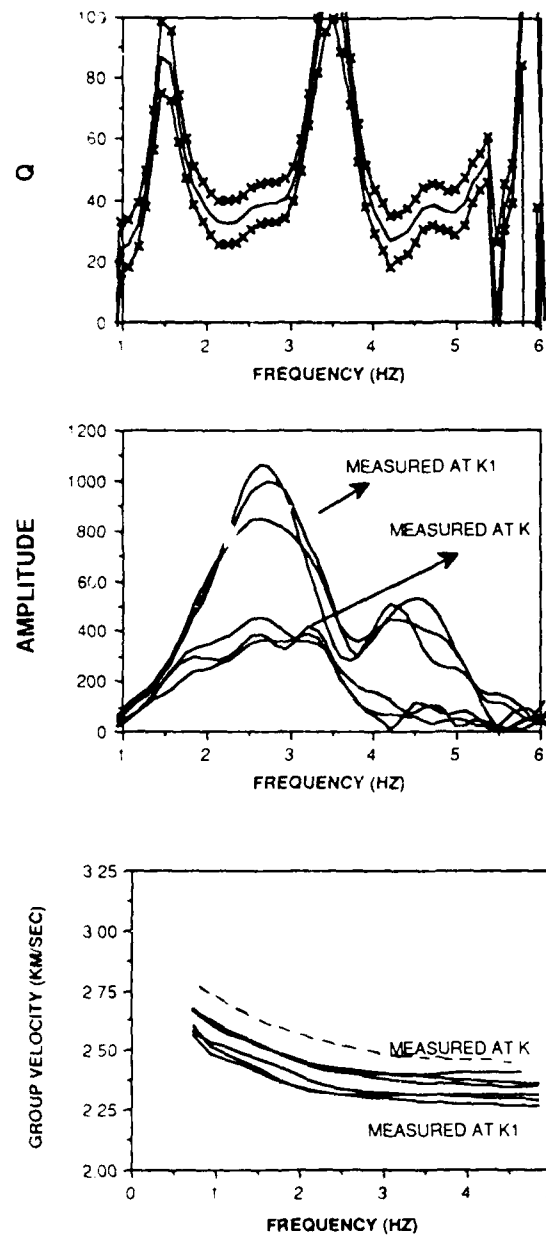


Figure 9. $Q(\omega)$, spectra and group velocities for regions K and K1. Dashed curve is the interstation group velocity used for Q determination.

before lateral heterogeneity is suspected.

An along strike attenuation curve was calculated for region L in Figure 7. In this $Q(\omega)$ determination an increase in Q is observed between 1 and 3 Hz and Q values of the same order as those observed for the cross strike regions are found (Figure 10). The increase in Q between 1 and 3 Hz could be due to lateral velocity variation, a frequency dependent $Q(\omega)$, or a low Q zone at depth. In theory a medium displaying an azimuthal dependence of velocity may also display an azimuthal dependence of attenuation. Although such behavior may exist, the effect is small enough to prevent unambiguous detection in the presence of lateral variations in velocity structure.

Figure 11 shows an average $Q(\omega)$ from all regions except between shots #15 to #4 and #15 to #16 where the Rg waves were too poorly developed to measure either group velocity or Q . The overall attenuation structure of the upper crust leads to surface wave $Q(\omega)$ values between 80 and 25. Delineation of the Q properties of individual mapped bedrock units is not possible due to the effect of lateral variations in velocity structure which violate the approximation of homogeneity assumed in the surface wave Q method. A dependence of attenuation on azimuth is predicted to exist but its effect cannot be observed in the presence of the previously discussed difficulties in Q measurements.

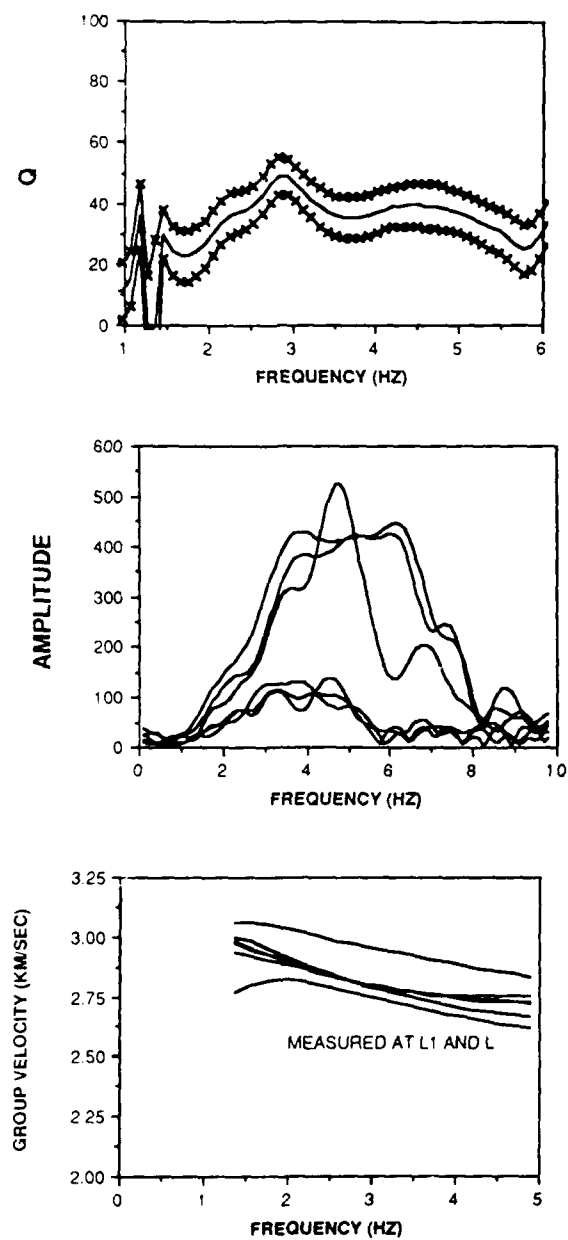


Figure 10. $Q(\omega)$, spectra and group velocities for regions L and L1.

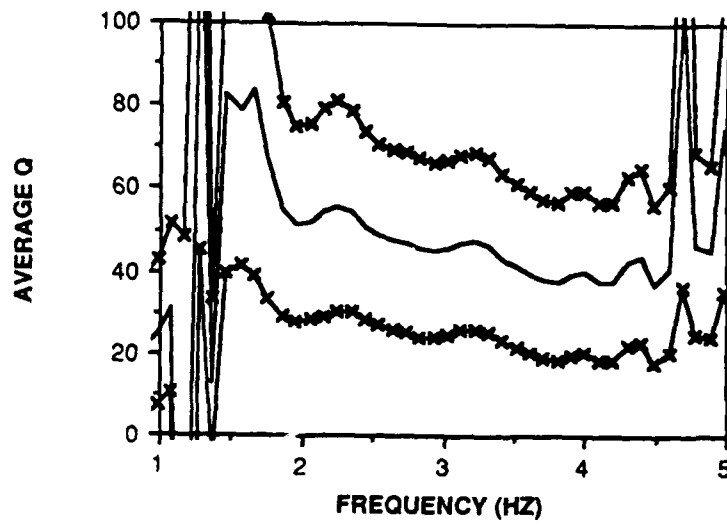


Figure 11. Average $Q(\omega)$ from all Q observations in this study.

INVERSION

A maximum likelihood inversion formulation discussed earlier is used to invert four sets of group velocity observations. This inversion assumes Gaussian distributions for the data observations and the initial model guess.

$$m_{k+1} = m_k + [A_k^T \cdot R_{dd} \cdot A_k + R_{mm}^{-1}]^{-1} \cdot [A_k^T \cdot R_{dd}^{-1} \cdot (d - G_k \cdot m_k) + (R_{mm})^{-1} \cdot (m_0 - m_k)] \quad (7)$$

In (7), m_k is the k th model, A_k is the k th sensitivity matrix, R_{dd} , R_{mm} are the data and model covariance matrices, G_k is the forward model relationship, and d is the data vector.

A data vector consisting of twenty-two group velocity observations between 0.9 and 5 Hz and a model composed of 14 layers each containing two parameters, the compressional (V_P) and shear (V_S) velocities, describe the inverse problem. Layering varies from 25 m thick very near the surface to 200 m thick at 1 km to 500 m thick at 2 km. Group velocity observations from regions A and B (Figure 1), presented earlier as evidence of lateral variation in velocity structure, are inverted for shear and compressional velocity structure. An along strike velocity structure is obtained by inverting group velocity observations from region H, and a cross strike structure is obtained by inverting group velocity curves from region G (Figure 1). These inversions assume isotropy and thus may not accurately describe certain regions in this study.

Schematic partial derivatives of group velocity with respect to V_P and V_S , from the final velocity model for region A, are shown in Figure 12. The shear velocity derivative dominates at depths greater than about (wavelength/5) but the magnitude of the compressional velocity derivative is sufficient near the surface to warrant its inclusion in the formulation of the inverse problem. Figure 12 clearly illustrates the depth limitations on the velocity inversion imposed by the lowest

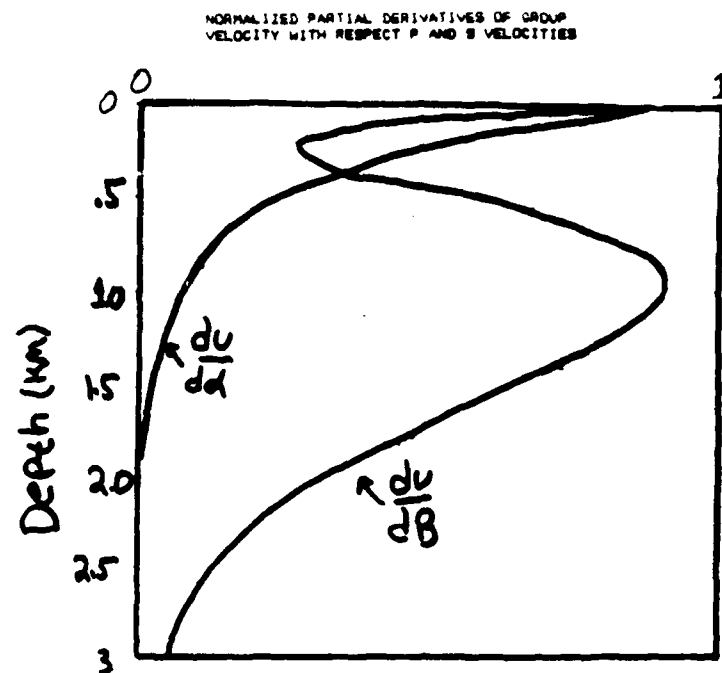


Figure 12. Partial derivatives of group velocity with respect to V_P and V_S for a 0.9 Hz Rayleigh wave using velocity model for region A.

observable frequency, in this case around 0.9 Hz.

The two group velocity curves from regions A and B and the inverted velocity models are shown in Figure 13. A shear velocity variation of 7 to 9% is found to exist between these two regions. Rows of the resolution matrix are plotted in Figure 14. A perfectly resolved parameter corresponds to a 1 on the diagonal and zeros elsewhere along the row corresponding to that parameter. The poorer the resolution the greater the deviation from this diagonalized delta function type behavior. The compressional velocities become poorly resolved at depth as is expected from Figure 12 and formally illustrated by Figure 14. The shear velocities are well resolved at all depths considered here. Compressional velocities determined from inversion of the group velocities agree well with *in situ* observations.

Along and cross strike velocity structures are found by inverting group velocities from regions G and H (Figures 15, 16). A difference of 15-20% is found to exist between these two velocity structures. A travel time curve was calculated from the compressional velocity model from the inversion and compared to the observed Pg travel time curve (Figure 17). The agreement between the predicted and the observed travel time curves is generally good. The theoretical travel time curve from the model for region G is systematically slower than the observations. The best fit compressional wave model for the data of Figure 17 is shown in Figure 15 as a dotted line and is compared to the compressional wave model from the surface wave inversion (solid line).

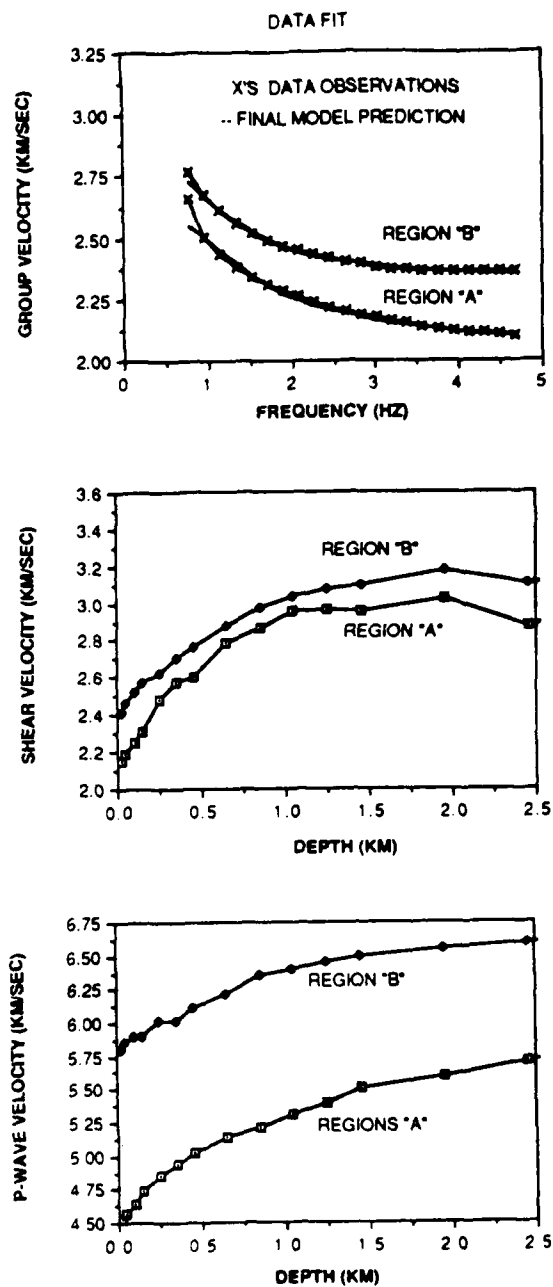
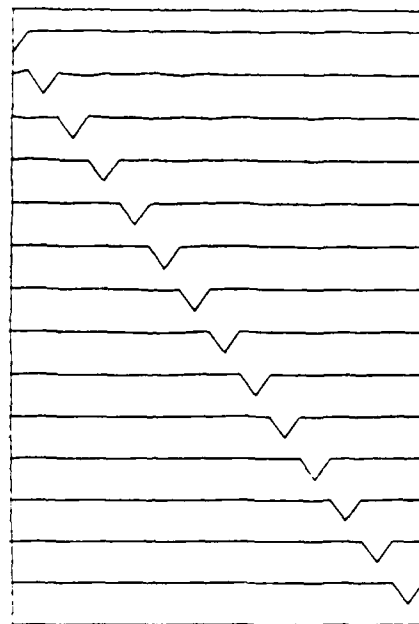


Figure 13. Velocity models for regions A and B and data fit. Each point in the velocity models corresponds to velocity in a given layer. Note evidence of lateral variation in velocity structure.

SHEAR VELOCITY RESOLUTION MATRIX



P VELOCITY RESOLUTION MATRIX

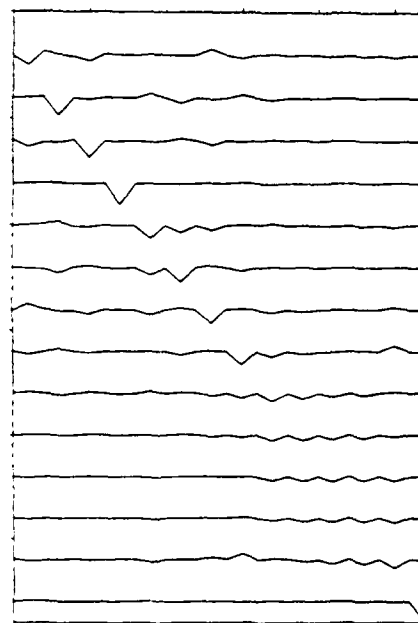


Figure 14. Resolution of shear and compressional velocity parameters, region A, represented as a plot of rows against columns of the resolution matrix. Each row corresponds to a model parameter, V_P or V_S , in a given layer. See Figure 13 for layer structure.

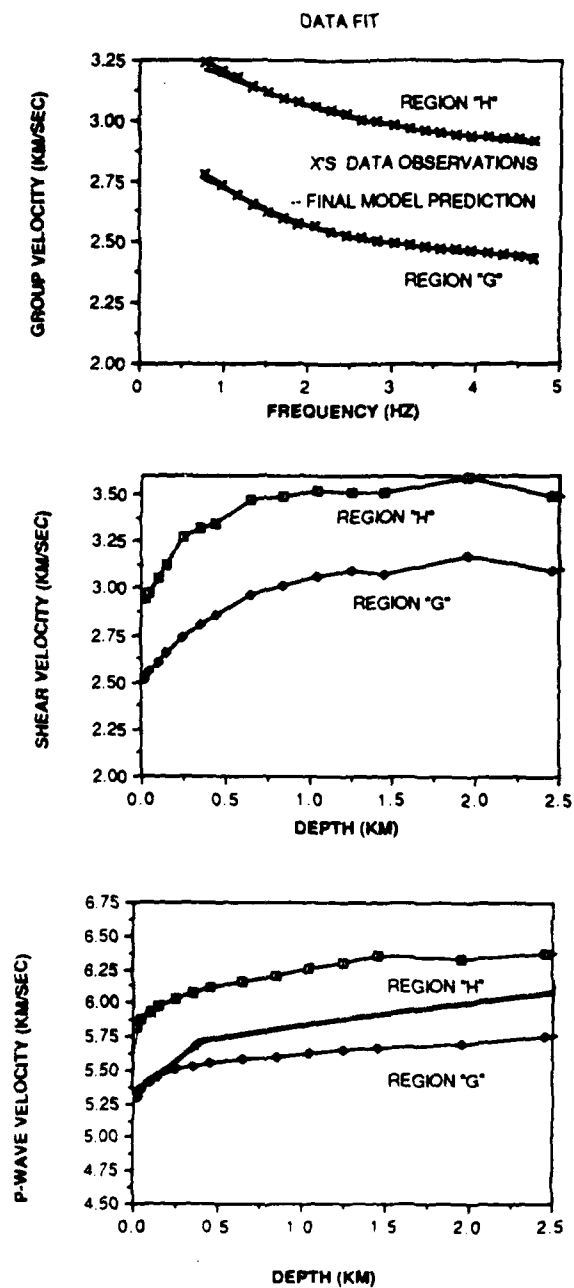
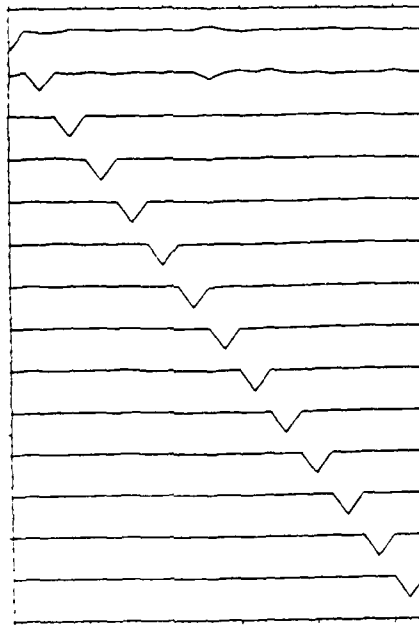


Figure 15. Velocity models for regions G and H and data fit. Dotted P-wave profile is derived by adjusting the velocity structure to match the observed Pg travel time curve. Note evidence of azimuthal variation of velocity. Each point in the velocity models corresponds to velocity in a given layer.

SHEAR VELOCITY RESOLUTION MATRIX



P VELOCITY RESOLUTION MATRIX

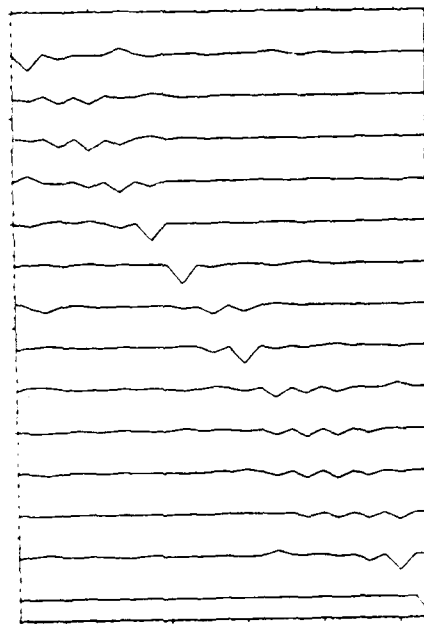


Figure 16. Resolution of shear and compressional velocity parameters, region H. Each row corresponds to a model parameter, V_P or V_S , in a given layer. See Figure 15 for layer structure.

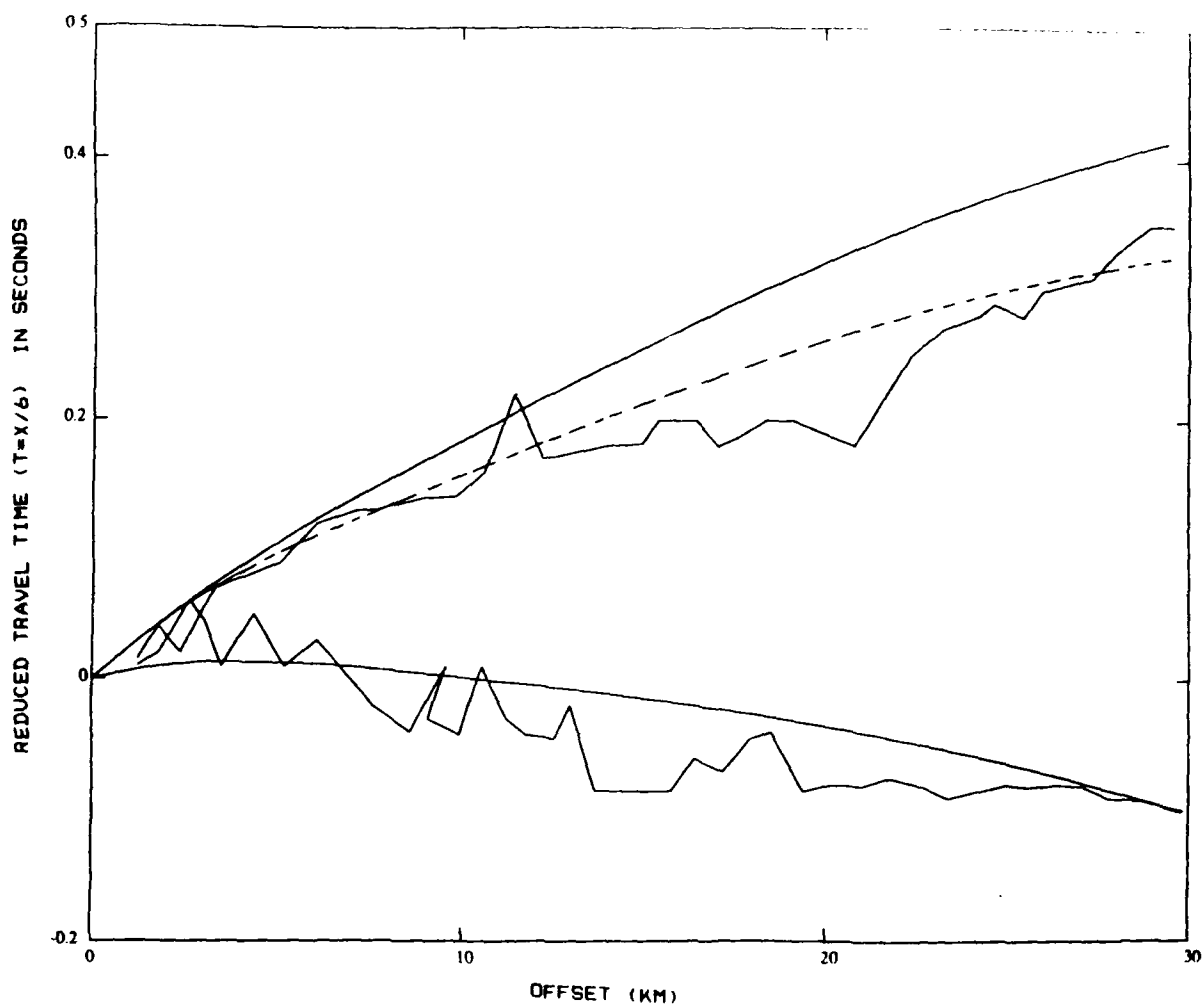


Figure 17. Comparison of observed Pg travel times with theoretical travel time curve from P-wave model from surface wave inversion (solid smooth curves). Dotted curve is best fitting model to travel time data after adjusting surface wave inversion model.

CONCLUSIONS

Lateral variations in velocity structure of up to 15% are observed from group velocity analysis of Rg waves and Pg velocities in southeastern Maine. Velocities determined from inversion of Rg group velocities agree generally with Pg velocities and the observed lateral variation in velocity correlates in some cases with mapped bedrock units and possibly tectonic features. A dependence of velocity on azimuth is observed for travel paths within the metasediments of the Central Merrimack Synclorium. Insufficient azimuthal coverage prevents a more accurate description of this observation but the magnitude of the observed velocity difference, up to 20%, coupled with the geology of the area suggest that anisotropy in the metasediments is a likely source of this velocity behavior. Lastly, the attenuation structure of the upper two kilometers of the crust is characterized by Q values between 25 and 80. Lateral variations in velocity structure prevent precise determinations of Q when using two station surface wave Q methods, but given the difficulties involved in upper crustal attenuation studies Rg waves provide a relatively stable estimate of Q structure.

REFERENCES

- Al-Husseini, M., J. Glover and B. Barley (1981). Dispersion patterns of the ground roll in eastern Saudi Arabia, *Geophysics* 46, 121-137.
- Anderson, J. and J. Dorman (1973). Local geological effects on short period Rayleigh waves around New York City, *Bull. Seis. Soc. Am.* 63, 1487-1497.
- Båth, M. (1975). Short period Rayleigh waves from near-surface events, *Phys. Earth Planet. Interiors* 10, 369-376
- Ben-Menahem, A. and S. Singh (1981). *Seismic Waves and Sources*, Springer-Verlag, New York
- Chen, T. and L. Alsop (1979). Reflection and transmission of obliquely incident Rayleigh waves at a vertical discontinuity between two welded quarter spaces, *Bull. Seis. Soc. Am.* 69, 1409-1424
- Dziewonski, A. and A. Hales (1972). Numerical analysis of dispersed seismic waves, in *Methods in Computational Physics* vol. 11, B. Bolt, Editor, Academic Press, New York, 39-85
- Dziewonski, A., S. Bloch and M. Landisman (1969). A technique for the analysis of transient seismic signals, *Bull. Seis. Soc. Am.* 59, 427-444
- Kafka, A. and M. Dollin (1985). Constraints on the lateral variation in upper crustal structure beneath southern New England from the dispersion of Rg waves, *Geophys. Res. Lett.* 12, 235-238.
- Kennett, B. (1984). Guided wave propagation in laterally varying media I. Theoretical development, *Geophys. J. Roy. Astron. Soc.* 79, 235-255
- Menke, W. (1984). *Geophysical Data Analysis: Discrete Inverse Theory*, Academic Press, London
- Murphy, J. M. and J. H. Luetgert (1986). Data report for the Maine-Quebec cross-strike seismic-

- refraction profile, *USGS Open-file Report 86-47*
- Murphy, J. M. and J. H. Luetgert (1987). Data report for the Maine-Quebec along-strike seismic-refraction profiles, *USGS Open-file Report 86-193*
- Papoulis, A. (1962). *The Fourier Integral and its Applications*, McGraw-Hill, New York
- Pulli, J. (1983). Seismicity, earthquake mechanisms, and seismic wave attenuation in the northeastern United States, *Ph.D. Thesis*, Massachusetts Institute of Technology
- Rodi, W., P. Glover, R. Li and S. Alexander (1975). A fast, accurate method for computing group-velocity partial derivatives for Rayleigh and Love waves, *Bull. Seis. Soc. Am.* 65, 1105-1114
- Takeuchi, H. and M. Saito (1972). Seismic surface waves, in *Methods in Computational Physics vol. 11*, B. Bolt, Editor, Academic Press, New York, 217-295
- Yomogida, K. (1985). Amplitude and phase variations of surface waves in a laterally heterogeneous earth: ray and beam theoretical approach, *Ph.D. Thesis*, Massachusetts Institute of Technology

CONTRACTORS (United States)

Professor Keiiti Aki
Center for Earth Sciences
University of Southern California
University Park
Los Angeles, CA 90089-0741

Professor Charles B. Archambeau
Cooperative Institute for Resch
in Environmental Sciences
University of Colorado
Boulder, CO 80309

Dr. Thomas C. Bache Jr.
Science Applications Int'l Corp.
10210 Campus Point Drive
San Diego, CA 92121 (2 copies)

Dr. Douglas R. Baumgardt
Signal Analysis & Systems Div.
ENSCO, Inc.
5400 Port Royal Road
Springfield, VA 22151-2388

Dr. S. Bratt
Science Applications Int'l Corp.
10210 Campus Point Drive
San Diego, CA 92121

Dr. Lawrence J. Burdick
Woodward-Clyde Consultants
P.O. Box 93245
Pasadena, CA 91109-3245 (2 copies)

Professor Robert W. Clayton
Seismological Laboratory/Div. of
Geological & Planetary Sciences
California Institute of Technology
Pasadena, CA 91125

Dr. Vernon F. Cormier
Department of Geology & Geophysics
U-45, Room 207
The University of Connecticut
Storrs, Connecticut 06268

Dr. Zoltan A. Der
ENSCO, Inc.
5400 Port Royal Road
Springfield, VA 22151-2388

Professor John Ferguson
Center for Lithospheric Studies
The University of Texas at Dallas
P.O. Box 830688
Richardson, TX 75083-0688

Professor Stanley Flatte'
Applied Sciences Building
University of California, Santa Cruz
Santa Cruz, CA 95064

Professor Steven Grand
Department of Geology
245 Natural History Building
1301 West Green Street
Urbana, IL 61801

Professor Roy Greenfield
Geosciences Department
403 Deike Building
The Pennsylvania State University
University Park, PA 16802

Professor David G. Harkrider
Seismological Laboratory
Div of Geological & Planetary Sciences
California Institute of Technology
Pasadena, CA 91125

Professor Donald V. Helmberger
Seismological Laboratory
Div of Geological & Planetary Sciences
California Institute of Technology
Pasadena, CA 91125

Professor Eugene Herrin
Institute for the Study of Earth
& Man/Geophysical Laboratory
Southern Methodist University
Dallas, TX 75275

Professor Robert B. Herrmann
Department of Earth & Atmospheric
Sciences
Saint Louis University
Saint Louis, MO 63156

Professor Lane R. Johnson
Seismographic Station
University of California
Berkeley, CA 94720

Professor Thomas H. Jordan
Department of Earth, Atmospheric
and Planetary Sciences
Mass Institute of Technology
Cambridge, MA 02139

Dr. Alan Kafka
Department of Geology &
Geophysics
Boston College
Chestnut Hill, MA 02167

Professor Leon Knopoff
University of California
Institute of Geophysics
& Planetary Physics
Los Angeles, CA 90024

Professor Charles A. Langston
Geosciences Department
403 Deike Building
The Pennsylvania State University
University Park, PA 16802

Professor Thorne Lay
Department of Geological Sciences
1006 C.C. Little Building
University of Michigan
Ann Harbor, MI 48109-1063

Dr. Randolph Martin III
New England Research, Inc.
P.O. Box 857
Norwich, VT 05055

Dr. Gary McCartor
Mission Research Corp.
735 State Street
P.O. Drawer 719
Santa Barbara, CA 93102 (2 copies)

Professor Thomas V. McEvilly
Seismographic Station
University of California
Berkeley, CA 94720

Dr. Keith L. McLaughlin
S-CUBED,
A Division of Maxwell Laboratory
P.O. Box 1620
La Jolla, CA 92038-1620

Professor William Menke
Lamont-Doherty Geological Observatory
of Columbia University
Palisades, NY 10964

Professor Brian J. Mitchell
Department of Earth & Atmospheric
Sciences
Saint Louis University
Saint Louis, MO 63156

Mr. Jack Murphy
S-CUBED
A Division of Maxwell Laboratory
11800 Sunrise Valley Drive
Suite 1212
Reston, VA 22091 (2 copies)

Professor J. A. Orcutt
Institute of Geophysics and Planetary
Physics, A-205
Scripps Institute of Oceanography
Univ. of California, San Diego
La Jolla, CA 92093

Professor Keith Priestley
University of Nevada
Mackay School of Mines
Reno, NV 89557

Wilmer Rivers
Teledyne Geotech
314 Montgomery Street
Alexandria, VA 22314

Professor Charles G. Sammis
Center for Earth Sciences
University of Southern California
University Park
Los Angeles, CA 90089-0741

Dr. Jeffrey L. Stevens
S-CUBED,
A Division of Maxwell Laboratory
P.O. Box 1620
La Jolla, CA 92038-1620

Professor Brian Stump
Institute for the Study of Earth & Man
Geophysical Laboratory
Southern Methodist University
Dallas, TX 75275

Professor Ta-liang Teng
Center for Earth Sciences
University of Southern California
University Park
Los Angeles, CA 90089-0741

Professor M. Nafi Toksoz
Earth Resources Lab
Dept of Earth, Atmospheric and
Planetary Sciences
Massachusetts Institute of Technology
42 Carleton Street
Cambridge, MA 02142

Professor Terry C. Wallace
Department of Geosciences
Building #11
University of Arizona
Tucson, AZ 85721

Weidlinger Associates
ATTN: Dr. Gregory Wojcik
620 Hansen Way, Suite 100
Palo Alto, CA 94304

Professor Francis T. Wu
Department of Geological Sciences
State University of new York
At Binghamton
Vestal, NY 13901

CTHERS (United States)

Dr. Monem Abdel-Gawad
Rockwell Internat'l Science Center
1049 Camino Dos Rios
Thousand Oaks, CA 91360

Professor Shelton S. Alexander
Geosciences Department
403 Deike Building
The Pennsylvania State University
University Park, PA 16802

Dr. Ralph Archuleta
Department of Geological
Sciences
Univ. of California at
Santa Barbara
Santa Barbara, CA

Dr. Muawia Barazangi
Geological Sciences
Cornell University
Ithaca, NY 14853

J. Barker
Department of Geological Sciences
State University of New York
at Binghamton
Vestal, NY 13901

Mr. William J. Best
907 Westwood Drive
Vienna, VA 22180

Dr. N. Biswas
Geophysical Institute
University of Alaska
Fairbanks, AK 99701

Dr. G. A. Bollinger
Department of Geological Sciences
Virginia Polytechnical Institute
21044 Derring Hall
Blacksburg, VA 24061

Dr. James Bulau
Rockwell Int'l Science Center
1049 Camino Dos Rios
P.O. Box 1085
Thousand Oaks, CA 91360

Mr. Roy Burger
1221 Serry Rd.
Schenectady, NY 12309

Dr. Robert Burrige
Schlumberger-Doll Resch Ctr.
Old Quarry Road
Ridgefield, CT 06877

Science Horizons, Inc.
ATTN: Dr. Theodore Cherry
710 Encinitas Blvd., Suite 101
Encinitas, CA 92024 (2 copies)

Professor Jon F. Claerbout
Professor Amos Nur
Dept. of Geophysics
Stanford University
Stanford, CA 94305 (2 copies)

Dr. Anton W. Dainty
AFGL/LWH
Hanscom AFB, MA 01731

Professor Adam Dziewonski
Hoffman Laboratory
Harvard University
20 Oxford St.
Cambridge, MA 02138

Professor John Ebel
Dept of Geology & Geophysics
Boston College
Chestnut Hill, MA 02167

Dr. Alexander Florence
SRI International
333 Ravenswood Avenue
Menlo Park, CA 94025-3493

Dr. Donald Forsyth
Dept. of Geological Sciences
Brown University
Providence, RI 02912

Dr. Anthony Gangi
Texas A&M University
Department of Geophysics
College Station, TX 77843

Dr. Freeman Gilbert
Institute of Geophysics &
Planetary Physics
Univ. of California, San Diego
P.O. Box 109
La Jolla, CA 92037

Mr. Edward Giller
Pacific Seifra Research Corp.
1401 Wilson Boulevard
Arlington, VA 22209

Dr. Jeffrey W. Given
Sierra Geophysics
11255 Kirkland Way
Kirkland, WA 98033

Dr. Henry L. Gray
Associate Dean of Dedman College
Department of Statistical Sciences
Southern Methodist University
Dallas, TX 75275

Rong Song Jih
Teledyne Geotech
314 Montgomery Street
Alexandria, Virginia 22314

Professor F.K. Lamb
University of Illinois at
Urbana-Champaign
Department of Physics
1110 West Green Street
Urbana, IL 61801

Dr. Arthur Lerner-Lam
Lamont-Doherty Geological Observatory
of Columbia University
Palisades, NY 10964

Dr. L. Timothy Long
School of Geophysical Sciences
Georgia Institute of Technology
Atlanta, GA 30332

Dr. Peter Malin
University of California at Santa Barbara
Institute for Central Studies
Santa Barbara, CA 93106

Dr. George R. Mellman
Sierra Geophysics
11255 Kirkland Way
Kirkland, WA 98033

Dr. Bernard Minster
Institute of Geophysics and Planetary
Physics, A-205
Scripps Institute of Oceanography
Univ. of California, San Diego
La Jolla, CA 92093

Dr. Geza Nagy
SRI International
333 Ravenswood Avenue
Menlo Park, CA 94025-3493

Dr. Jack Oliver
Department of Geology
Cornell University
Ithaca, NY 14850

Dr. Robert Phinney/Dr. F.A. Dahlen
Dept of Geological
Geophysical Sci. University
Princeton University
Princeton, NJ 08540 (2 copies)

RADIX Systems, Inc.
Attn: Dr. Jay Pulli
2 Taft Court, Suite 203
Rockville, Maryland 20850

Professor Paul G. Richards
Lamont-Doherty Geological
Observatory of Columbia Univ.
Palisades, NY 10964

Dr. Norton Rimer
S-CUBED
A Division of Maxwell Laboratory
P.O. 1620
La Jolla, CA 92038-1620

Professor Larry J. Ruff
Department of Geological Sciences
1006 C.C. Little Building
University of Michigan
Ann Arbor, MI 48109-1063

Dr. Alan S. Ryall, Jr.
Center of Seismic Studies
1300 North 17th Street
Suite 1450
Arlington, VA 22209-2308 (4 copies)

Dr. Richard Sailor
TASC Inc.
55 Walkers Brook Drive
Reading, MA 01867

Dr. David G. Simpson
Lamont-Doherty Geological Observ.
of Columbia University
Palisades, NY 10964

Dr. Bob Smith
Department of Geophysics
University of Utah
1400 East 2nd South
Salt Lake City, UT 84112

Dr. S. W. Smith
Geophysics Program
University of Washington
Seattle, WA 98195

Rondout Associates
ATTN: Dr. George Sutton,
Dr. Jerry Carter, Dr. Paul Pomeroy
P.O. Box 224
Stone Ridge, NY 12484 (4 copies)

Dr. L. Sykes
Lamont Doherty Geological Observ.
Columbia University
Palisades, NY 10964

Dr. Pradeep Talwani
Department of Geological Sciences
University of South Carolina
Columbia, SC 29208

Dr. R. B. Tittmann
Rockwell International Science Center
1049 Camino Dos Rios
P.O. Box 1085
Thousand Oaks, CA 91360

Professor John H. Woodhouse
Hoffman Laboratory
Harvard University
20 Oxford St.
Cambridge, MA 02138

Dr. Gregory B. Young
ENSCO, Inc.
5400 Port Royal Road
Springfield, VA 22151-2388

OTHERS (FOREIGN)

Dr. Peter Basham
Earth Physics Branch
Geological Survey of Canada
1 Observatory Crescent
Ottawa, Ontario
CANADA K1A 0Y3

Dr. Eduard Berg
Institute of Geophysics
University of Hawaii
Honolulu, HI 96822

Dr. Michel Bouchon - Universite
Scientifique et Medicale de Grenob
Lab de Geophysique - Interne et
Tectonophysique - I.R.I.G.M.-B.P.
38402 St. Martin D'Herès
Cedex FRANCE

Dr. Hilmar Bungum/NTNF/NORSAR
P.O. Box 51
Norwegian Council of Science,
Industry and Research, NORSAR
N-2007 Kjeller, NORWAY

Dr. Michel Campillo
I.R.I.G.M.-B.P. 68
38402 St. Martin D'Herès
Cedex, FRANCE

Dr. Kin-Yip Chun
Geophysics Division
Physics Department
University of Toronto
Ontario, CANADA M5S 1A7

Dr. Alan Douglas
Ministry of Defense
Blacknest, Brimpton,
Reading RG7-4RS
UNITED KINGDOM

Dr. Manfred Henger
Fed. Inst. For Geosciences & Nat'l Res.
Postfach 510153
D-3000 Hannover 51
FEDERAL REPUBLIC OF GERMANY

Dr. E. Husebye
NTNF/NORSAR
P.O. Box 51
N-2007 Kjeller, NORWAY

Tormod Kvaerna
NTNF/NORSAR
P.O. Box 51
N-2007 Kjeller, NORWAY

Mr. Peter Marshall, Procurement
Executive, Ministry of Defense
Blacknest, Brimpton,
Reading FG7-4RS
UNITED KINGDOM (3 copies)

Dr. Ben Menaheim
Weizman Institute of Science
Rehovot, ISRAEL 951729

Dr. Svein Mykkeltveit
NTNF/NORSAR
P.O. Box 51
N-2007 Kjeller, NORWAY (3 copies)

Dr. Robert North
Geophysics Division
Geological Survey of Canada
1 Observatory crescent
Ottawa, Ontario
CANADA, K1A 0Y3

Dr. Frode Ringdal
NTNF/NORSAR
P.O. Box 51
N-2007 Kjeller, NORWAY

Dr. Jorg Schlittenhardt
Federal Inst. for Geosciences & Nat'l Res.
Postfach 510153
D-3000 Hannover 51
FEDERAL REPUBLIC OF GERMANY

University of Hawaii
Institute of Geophysics
ATTN: Dr. Daniel Walker
Honolulu, HI 96822

FOREIGN CONTRACTORS

Dr. Ramon Cabre, S.J.
c/o Mr. Ralph Buck
Economic Consular
American Embassy
APO Miami, Florida 34032

Professor Peter Harjes
Institute for Geophysik
Rhur University/Bochum
P.O. Box 102148 4630 Bochum 1
FEDERAL REPUBLIC OF GERMANY

Professor Brian L.N. Kennett
Research School of Earth Sciences
Institute of Advanced Studies
G.P.O. Box 4
Canberra 2601
AUSTRALIA

Dr. B. Massinon
Societe Radiomana
27, Rue Claude Bernard
75005, Paris, FRANCE (2 copies)

Dr. Pierre Mechler
Societe Radiomana
27, Rue Claude Bernard
75005, Paris, FRANCE

GOVERNMENT

Dr. Ralph Alewine III
DARPA/NMRO
1400 Wilson Boulevard
Arlington, VA 22209-2308

Dr. Peter Basham
Geological Survey of Canada
1 Observatory Crescent
Ottawa, Ontario
CANADA K1A 0Y3

Dr. Robert Blandford
DARPA/NMRO
1400 Wilson Boulevard
Arlington, VA 22209-2308

Sandia National Laboratory
ATTN: Dr. H. B. Durham
Albuquerque, NM 87185

Dr. Jack Evernden
USGS-Earthquake Studies
345 Middlefield Road
Menlo Park, CA 94025

U.S. Geological Survey
ATTN: Dr. T. Hanks
Nat'l Earthquake Resch Center
345 Middlefield Road
Menlo Park, CA 94025

Dr. James Hannon
Lawrence Livermore Nat'l Lab.
P.O. Box 808
Livermore, CA 94550

U.S. Arms Control & Disarm. Agency
ATTN: Dick Morrow
Washington, D.C. 20451

Paul Johnson
ESS-4, Mail Stop J979
Los Alamos National Laboratory
Los Alamos, NM 87545

Ms. Ann Kerr
DARPA/NMRO
1400 Wilson Boulevard
Arlington, VA 22209-2308

Dr. Max Koontz
US Dept of Energy/DP 331
Forrestal Building
1000 Independence Ave.
Washington, D.C. 20585

Dr. W. H. K. Lee
USGS
Office of Earthquakes, Volcanoes,
& Engineering
Branch of Seismology
345 Middlefield Rd
Menlo Park, CA 94025

Dr. William Leith
USGS
Mail Stop 928
Reston, VA 22092

Dr. Robert Masse'
Box 25046, Mail Stop 967
Denver Federal Center
Denver, Colorado 80225

R. Morrow
ACDA/VI
Room 5741
320 21st Street N.W
Washington, D.C. 20451

Dr. Keith K. Nakanishi
Lawrence Livermore National Laboratory
P.O. Box 808, L-205
Livermore, CA 94550 (2 copies)

Dr. Carl Newton
Los Alamos National Lab.
P.O. Box 1663
Mail Stop C335, Group E553
Los Alamos, NM 87545

Dr. Kenneth H. Olsen
Los Alamos Scientific Lab.
Post Office Box 1663
Los Alamos, NM 87545

Howard J. Patton
Lawrence Livermore National Laboratory
P.O. Box 808, L-205
Livermore, CA 94550

AFOSR/NP
ATTN: Colonel Jerry J. Perrizo
Bldg 410
Bolling AFB, Wash D.C. 20332-6448

HQ AFTAC/TT
Attn: Dr. Frank F. Pilotte
Patrick AFB, Florida 32925-6001

Mr. Jack Rachlin
USGS - Geology, Rm 3 C136
Mail Stop 928 National Center
Reston, VA 22092

Robert Reinke
AFWL/NTESC
Kirtland AFB, NM 87117-6008

HQ AFTAC/TCR
Attn Dr. George H. Rothe
Patrick AFB, Florida 32925-6001

Donald L. Springer
Lawrence Livermore National Laboratory
P.O. Box 808, L-205
Livermore, CA 94550

Dr. Lawrence Turnbull
OSWR/NED
Central Intelligence Agency
CIA, Room 5G48
Washington, D.C. 20505

Dr. Thomas Weaver
Los Alamos Scientific Laboratory
Los Alamos, NM 97544

AFGL/SULL
Research Library
Hanscom AFB, MA 01731-5000 (2 copies)

Secretary of the Air Force (SAFRD)
Washington, DC 20330
Office of the Secretary Defense
DDR & E
Washington, DC 20330

HQ DNA
ATTN: Technical Library
Washington, DC 20305

Director, Technical Information
DARPA
1400 Wilson Blvd.
Arlington, VA 22209

AFGL/XO
Hanscom AFB, MA 01731-5000

AFGL/LW
Hanscom AFB, MA 01731-5000

DARPA/PM
1400 Wilson Boulevard
Arlington, VA 22209

Defense Technical
Information Center
Cameron Station
Alexandria, VA 22314
(12 copies)

Defense Intelligence Agency
Directorate for Scientific &
Technical Intelligence
Washington, D.C. 20301

Defense Nuclear Agency/SPSS
ATTN: Dr. Michael Shore
6801 Telegraph Road
Alexandria, VA 22310

AFTAC/CA (STINFO)
Patrick AFB, FL 32925-6001